Centripetal Retinal Degeneration Follows an Exponential Decay and May Be Reversed Following Gene Therapy

MARAM E.A. ABDALLA ELSAYED, AMANDEEP S. JOSAN, SALWAH REHMAN, AND ROBERT E. MACLAREN

• PURPOSE: To model the progression of the hyperautofluorescent ring in rod-cone dystrophies and to report a novel finding of its reversal following gene therapy.
• DESIGN: Retrospective analysis of a prospective cohort study.
• PARTICIPANTS: Fifty-eight individuals with genotyped rod-cone dystrophies and hyperautofluorescent rings on fundus autofluorescence (FAF).
• METHODS: Patients with a rod-cone dystrophy and hyperautofluorescent rings on FAF were identified and their rings categorized according to disease progression. Correlation between different FAF and optical coherence tomography (OCT) parameters in patients with early-mid stage disease were calculated. A retrospective, longitudinal analysis of FAF images was subsequently performed. A linear mixed model, with the dependent variable of total horizontal hyperautofluorescent ring width and independent variables of time, genotype and the interactions was used.
• MAIN OUTCOME MEASURES: Horizontal diameter of the hyperautofluorescent ring.
• RESULTS: A total of 58 rod-cone dystrophy patients were analyzed in this study. Twenty eyes of 20 patients presented with early to mid-stage disease. The internal ring diameter, external ring diameter and ring thickness, were strongly correlated with the ellipsoid zone width ($r = 0.94$), external limiting membrane width ($r = 0.97$) and loss of the ellipsoid zone ($r = 0.92$) respectively. Longitudinal analysis suggests that FAF changes decline very predictably in a logarithmic fashion ($R^2 = 0.958$). Results indicated a significant reversal of the hyperautofluorescent ring following RPGR gene therapy (using Cotoretigene Toliparvovec), correlating with improvements in retinal sensitivity.
• CONCLUSIONS: Our findings suggest that centripetal retinal degeneration in rod-cone dystrophies follows an exponential decay and that gene therapy may reverse both structural and functional deficits. (Am J Ophthalmol 2026;289: 76–86. © 2026 Published by Elsevier Inc. This is an open access article under the CC BY license (http://creativecommons.org/licenses/by/4.0/))

INTRODUCTION

Fundus autofluorescence (FAF) imaging is based on detecting physiologically and pathologically occurring fluorophores primarily in the photoreceptors and retinal pigment epithelium (RPE) to map the metabolic profile of the fundus. Incomplete lysosomal degradation of shed photoreceptor outer segments by the RPE results in the accumulation of lipofuscin within the retinal pigment epithelial cells - a major contributor to FAF. Distinct changes in retinal FAF are seen in rod-cone dystrophies and correlate with loss of the overlying photoreceptors.[1] Fundus autofluorescence intensity largely depends upon the concentration of lipofuscin in the retinal pigment epithelium (RPE). Rod-cone dystrophies typically result in midperipheral loss of visual field, which correlates closely with the photoreceptor degeneration as it progresses from the periphery. On imaging with FAF, this zone of partially degenerate photoreceptors can be identified by a hyperautofluorescent ring, particularly in ciliopathies (Figure 1). Prior research has expanded our understanding of the FAF response, demonstrating that its boundary delineates the area of transition between the normal and diseased retina.[2,3] In addition, studies have found that progressive constriction of the hyperautofluorescent ring correlates with visual field and full-field electroretinogram data, demonstrating deteriorating visual function.[2,4-6] Rod-cone dystrophies may especially be suited for evaluation with FAF, as a deep-learning neural network was able to distinguish between rod-cone dystrophies and healthy retinas with an accuracy of 95% based on FAF alone.[7] Hence, FAF measures may be a potential biomarker in gene therapy clinical trials for monitoring changes in early disease, when visual acuity is still minimally affected. For FAF to serve as a clinically useful biomarker of rod-cone

AJO.com Supplemental Material available at AJO.com.
Accepted for publication May 19, 2026.
From the Nuffield Laboratory of Ophthalmology (M.E.A.A.E., A.S.J., S.R., R.E.M.), Department of Clinical Neurosciences, University of Oxford, Oxford, UK; Oxford Eye Hospital (M.E.A.A.E., A.S.J., S.R., R.E.M.), Oxford University Hospitals NHS Foundation Trust, Oxford, UK
Inquiries to Robert E Maclaren, Nuffield Laboratory of Ophthalmology, Department of Clinical Neurosciences, University of Oxford, Oxford, UK.; e-mail: enquiries@eye.ox.ac.uk

0002-9394/$36.00
https://doi.org/10.1016/j.ajo.2026.05.029

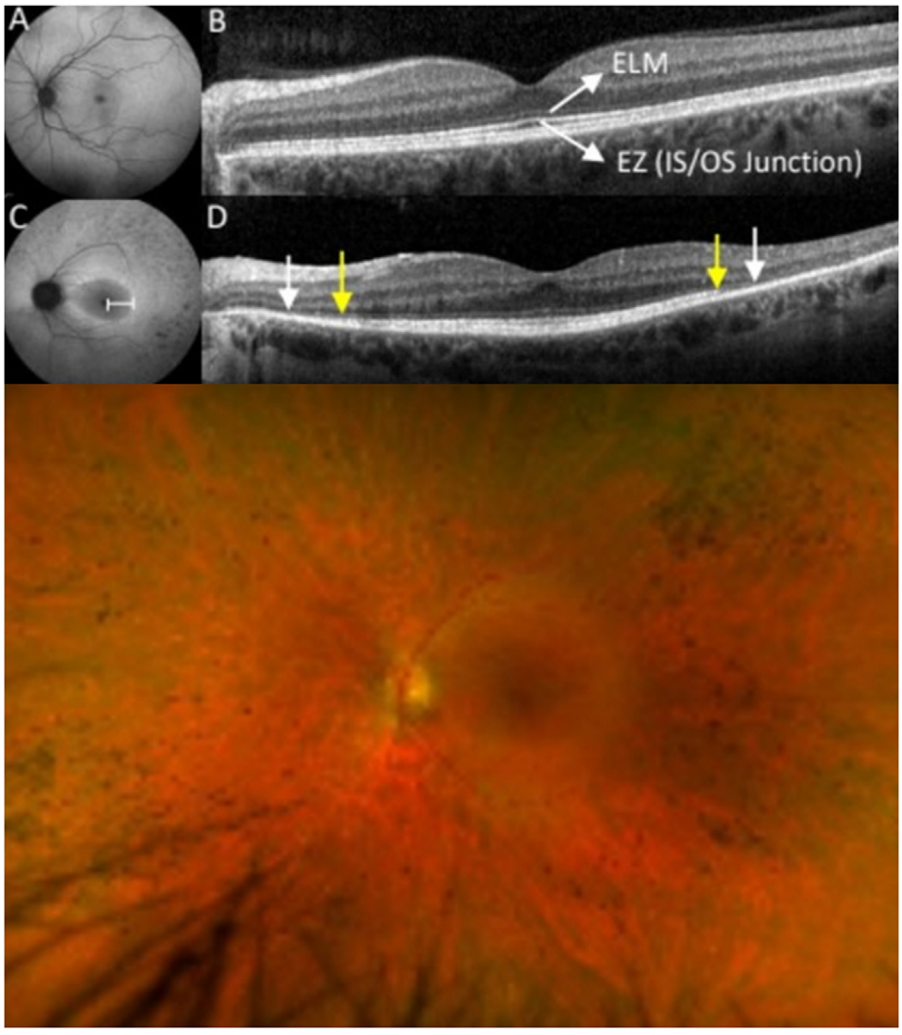

FIGURE 1. Retinal imaging in a control eye (A, B) and a patient with RPGR -/y dystrophy (C, D). Fundus autofluorescence demonstrating a hyperautofluorescent ring surrounding the macula (C). Optical coherence tomography showing (B) a cross-sectional image of the central macula in the control eye; (D) the limits of the inner-outer segment (IS/OS) junction (arrows) corresponding to the area within the hyperautofluorescent zone. The yellow arrows indicate the termination of the ellipsoid zone. The white arrows denote the end of the external limiting membrane. (E) Pseudo-colour Optos image of the right eye of a patient with RPGR-/y.

dystrophy disease progression, it should be related to structural measures of photoreceptor loss. It has previously been shown through a cross-sectional analysis of a group of individuals at different stages of disease, that FAF changes follow an exponential decay over time for patients with choroideremia, an RPE disease.[8] However, this exponential decay can only be inferred when studying a cross-sectional group of patients and the possibility exists that the true decay function in any one individual followed for many years may deviate significantly from this inference. Therefore, in order to effectively track disease progression and target disease characteristics at an individual level, knowledge of how FAF progresses through a longitudinal analysis is more relevant than a cross-sectional analysis. An exponential model has been proposed as a potential method for estimating the evolution of the autofluorescent area in retinitis pigmentosa patients.[9] However, genetic diagnosis was not conducted for the entire group of individuals in this cohort, thus requiring additional investigation.

The aim of the present longitudinal study was to investigate the relationship between optical coherence tomography (OCT) anatomical measures of photoreceptor loss with FAF measures and to investigate FAF changes over time in individuals with rod-cone dystrophies (predominantly ciliopathies) characterized by photoreceptor outer segment loss preceding the inner segments. Photoreceptor outer segments require efficient transport of phototransduction proteins via the connecting cilium. It is unknown whether the degeneration of these disorders would follow an exponential decay function, similar to choroideremia, which is a disease of the RPE.

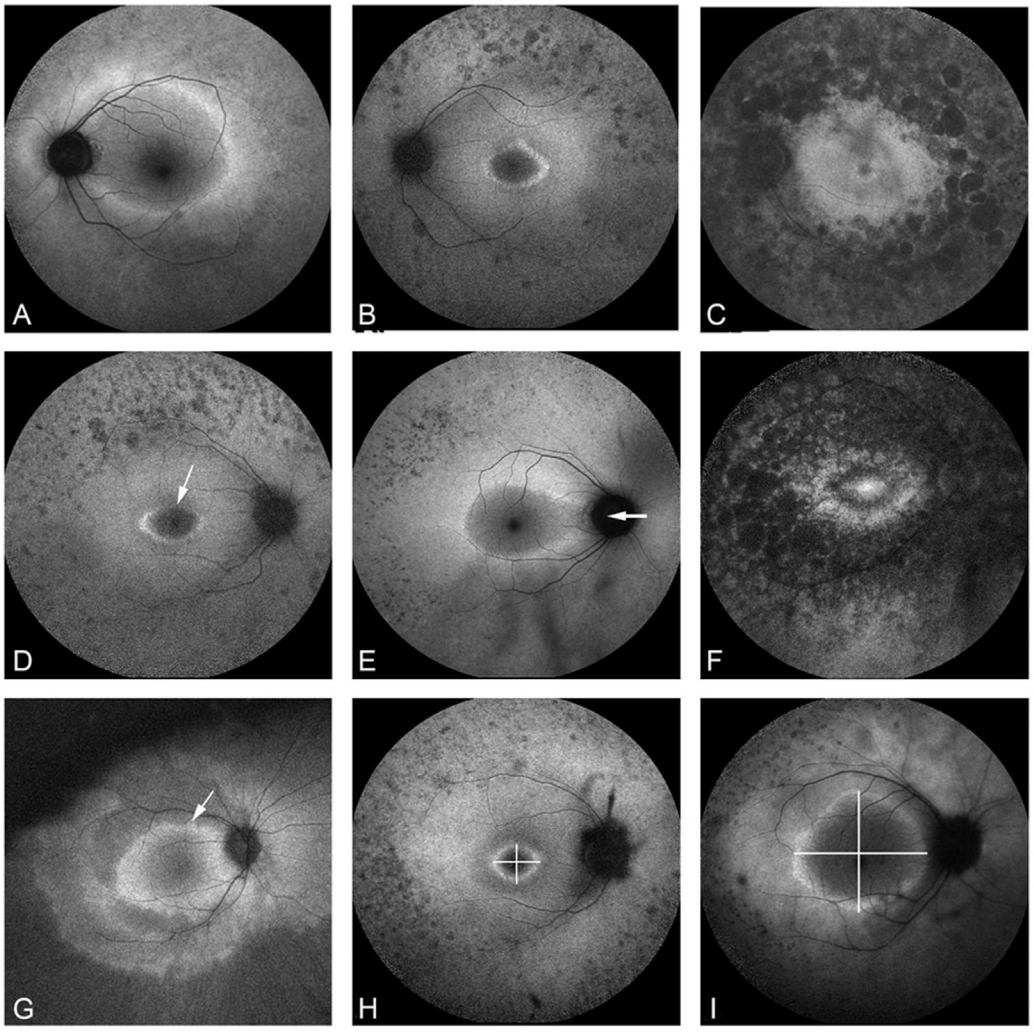

FIGURE 2. (A) Early-stage large hyperautofluorescent ring involving the optic disc, (B) Mid-stage circumferential hyperautofluorescent ring around the fovea, and (C) Late- stage pattern of diffuse, irregular hyperautofluoresence in the central macula. (D, E) Patients excluded from the study as the horizontal or vertical diameters could not be measured due to missing portions of the hyperautofluorescent ring. Arrows demonstrate the poorly defined superior (D) and nasal (E) aspects. (F) Patients excluded due to poorly defined ring. (G) When a double ring was present, the internal ring was measured. (H, I) Vertical and horizontal measurements across the fovea of an elliptical and nonelliptical hyperautofluorescent ring.

METHODS

• **SUBJECTS:** We identified 58 consecutive patients who had rod-cone dystrophy and hyperautofluorescent rings on FAF retrospectively from our clinical database and categorized the rings according to disease progression. Three distinct stages of ring were evident; early, mid or late-stage disease (Figure 2A-C). An early stage ring is one that extends into the nasal retina and envelops the optic disc. The mid-stage ring is the classic shape seen when photoreceptor density shifts from rod-dominant to cone-dominant and can sometimes adopt a "bullseye" pattern. In late-stage disease, there are diffuse autofluorescence changes within the central cone-rich area. Here, there is significant disruption of the retinal anatomy and structural correlations are more challenging. No cases of unilateral or X-linked rod-cone dystrophy in female patients were included in the study.

For the cross-sectional analysis, we included patients with early-mid stage ring phenotypes in whom the ring borders were measurable (horizontal and/or vertical diameter across the fovea) and with analyzable OCT for EZ/ELM metrics. This yielded a cross-sectional cohort of 29 patients. For the longitudinal analysis, we then restricted the cross-sectional cohort to patients with ≥3 clinic visits with FAF suitable for registered repeat measurements. Twenty patients (mean age 42.2 years; range 11.0-76.0 years) met this requirement and were included in the longitudinal progression analysis, while 9/29 were excluded because they had fewer than 3 follow-up visits.

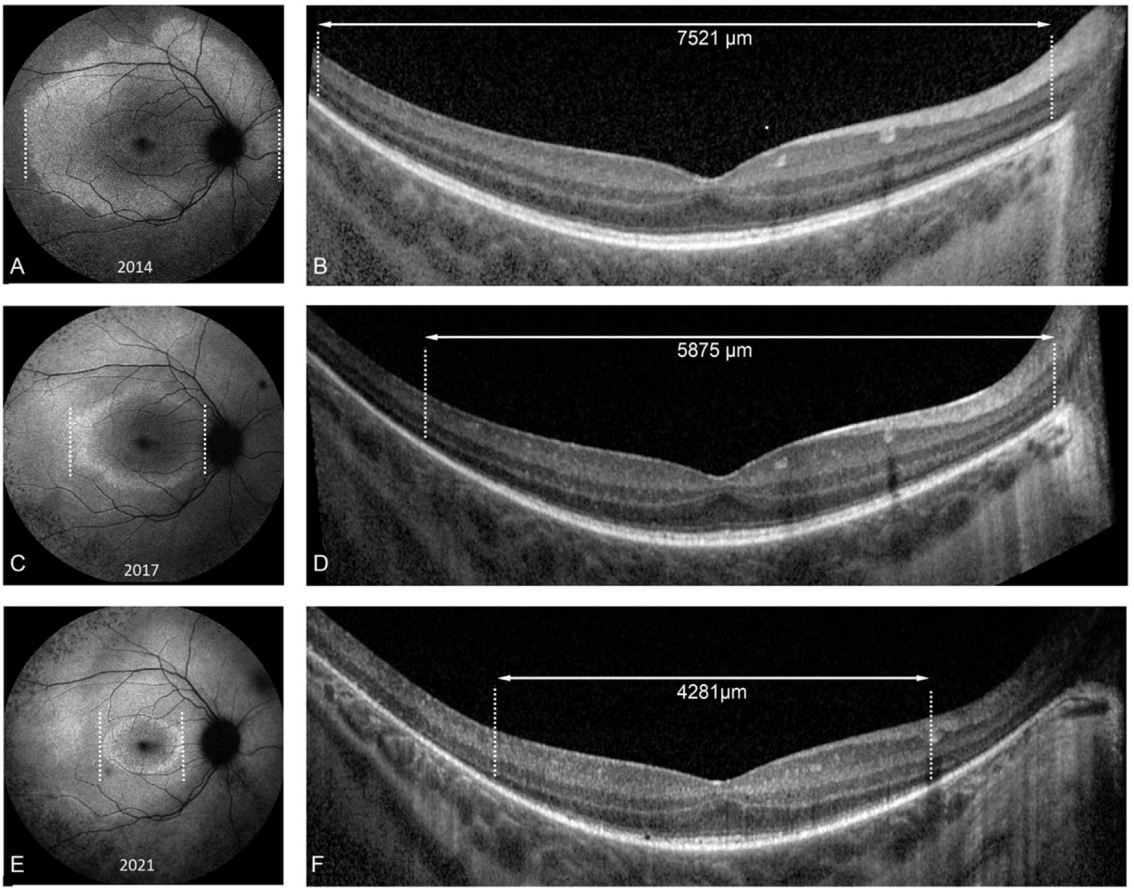

FIGURE 3. Fundus autofluorescence and optical coherence tomography images monitoring progression over time. Dashed lines indicate the width of hyperautofluorescent ring. White lines indicate the width of the ellipsoid zone on OCT. With progression from early to mid-stage disease there is progressive constriction of the hyperautofluorescent ring and the ellipsoid line width.

Baseline and subsequent hyperautofluorescent ring parameters were evaluated. Patients had undergone a full consultative ophthalmic examination at the Oxford Eye Hospital. Clinical data and genetic testing were performed as part of routine clinical care and data and results were collected retrospectively. For this analysis, patients with a clinical diagnosis of a rod-cone dystrophy confirmed on molecular genetic testing and who had images with a distinct macular hyperautofluorescent ring were included. Patients with ocular co-pathologies were excluded from the study.

• **TESTING PROTOCOLS:** Patients had undergone a standardized imaging protocol consisting of pseudo-colour fundus Optos images (Optomap P200; Optos plc, Dunfermline, UK) and spectral-domain optical coherence tomography (Spectralis, Heidelberg Engineering, Inc., Heidelberg, Germany). Fundus autofluorescence imaging was performed with a 30° and 55° field of view using a 488-nm excitation Spectralis confocal scanning laser ophthalmoscope (Heidelberg Engineering, Heidelberg, Germany) after pupil dilation with topical 0.5% tropicamide and 2.5% phenylephrine. Each image of a series was checked for optimal image quality. Images were excluded in cases of inhomogeneous illumination, sectorial opacities (e.g., eyelashes, floater), or unstable fixation. OCT follow-up images were co-registered to the baseline scan location using the device's follow-up functionality. The right eye was used for analysis. If not applicable (for example, due to poor image quality or anatomical abnormalities), the left eye was used instead. The width of the ellipsoid zone (EZ) and external limiting membrane (ELM) were measured from spectral domain optical coherence tomography (OCT), Figure 1. On the SD-OCT, the nasal and temporal edges of the EZ line were defined as the locations where the EZ line met the RPE. The width of the EZ line was defined as the distance between these 2 locations at the fovea. Patients were excluded from the study if the horizontal or vertical diameters could not be measured due to missing portions of the hyperautofluorescent ring (Figure 2D, E) or a very poorly defined ring (Figure 2F). When a double ring was present, the internal ring was measured. The FAF images were analyzed using measurements of horizontal hyperautofluorescent ring diameter across the fovea (Figure 2H). The vertical diameter was considered to be the line crossing the foveal center

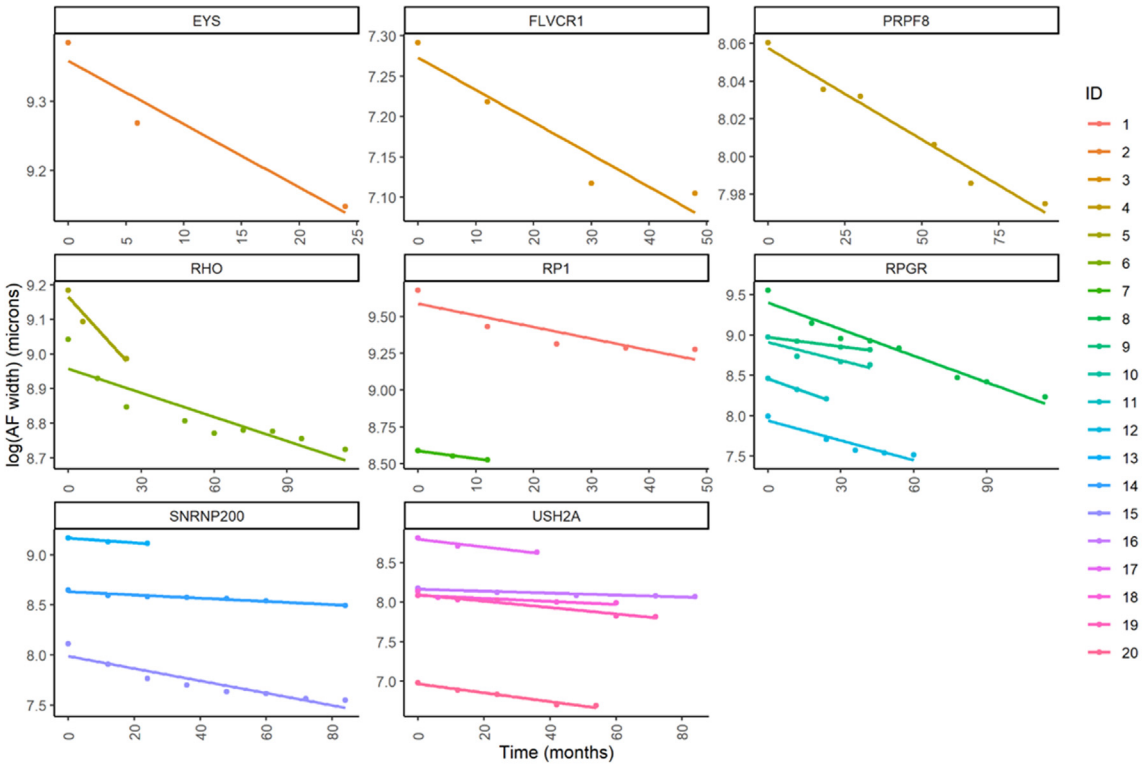

FIGURE 4. Hyperautofluorescent ring diameter decay over time for different patients with different genetic mutations. Linear mixed models which included time and the factor in question, using an interaction between time and the potential factor as predictors. The ring diameter fits an exponential decay function (R2 = 0.995; *P* < 0.001). Age and sex had no statistically significant effect on the exponential decay function.

and perpendicular to the horizontal diameter even in cases where the ring was nonelliptical (Figure 2I). The measurement of the horizontal and vertical autofluorescence ring diameter were demarcated by the external delineable boundary. This was done manually. It should be noted that the ring thickness can be added to the inner ring diameter to get the outer ring diameter. In cases involving the nasal edge of the hyperautofluorescent falling outside the optic nerve, the diameter was still measured across the fovea and extended beyond the optic nerve. All measurements were done by 2 independent graders (MAE and SR).

The boundaries of the hyperautofluorescent ring were measured using the measuring tool included in the Spectralis Software. This was chosen as it is a simple and repeatable method. Measurements from follow-up visits were transferred onto the baseline image using the internal image registration function of HEYEX (Heidelberg, Germany), thereby overcoming discrepancies arising from small changes in focus, orientation, and edge distortion. Measurements of the horizontal hyperautofluorescent ring diameter were used, as opposed to the vertical axis, for 2 reasons. First, being the greater distance, measurement error and measurement variation between observers would be expected to have a smaller effect. Second, at matched eccentricity, it is observed that visual performance along the horizontal meridian outperforms the vertical visual meridian, suggesting that this meridian provides a more important role in human visual function and behaviour.[10] The presence of polar angle asymmetries has been recognised in various visual tasks, including those involving contrast sensitivity,[11-13] spatial resolution,[13,14] and tasks that engage higher visual areas, such as visual working memory. IRB/Ethics Committee ruled that approval was not required for this study.

Microperimetry was performed using the Macular Integrity Assessment (MAIA) confocal microperimeter (CenterVue, Padova, Italy) using the 10-2 grid and <=30% fixation losses reliability criteria.

Ethics approval was not needed for the retrospective audit of pseudoanoymised images; however, the gene therapy trial (ClinicalTrials.gov identifier, NCT03116113) was previously approved with NightstaRx Ltd as the sponsor.

• **STATISTICAL ANALYSIS:** Statistical analysis was performed using R 4.2.1 (R Foundation for Statistical Computing, Vienna, Austria) using the lme4 package (Bates, 2015). Normality was assessed using visual inspection of q-q plots and homogeneity of variances was assessed using a residual plot. All statistical tests were two-tailed with an alpha significance level set at 0.05. Pearson correlation coefficient was used as a measure of the strength of correlation of OCT parameters and ring radius.

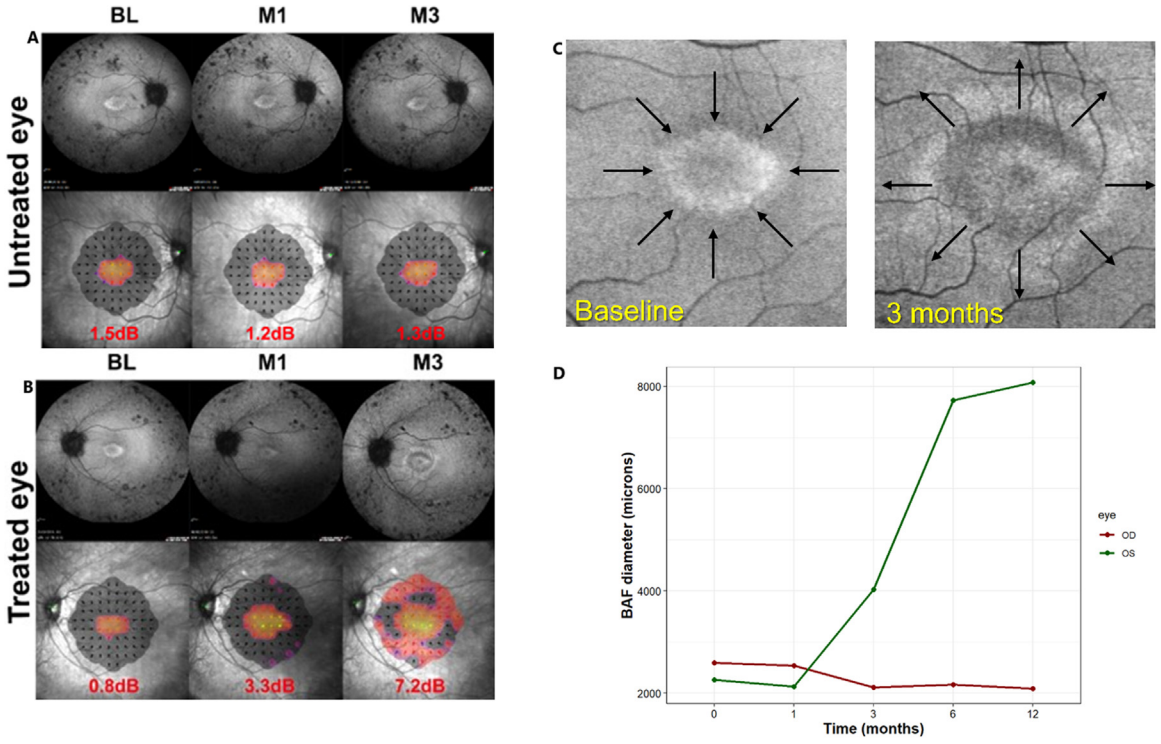

FIGURE 5. Reversal of the hyperautofluorescent ring following RPGR gene therapy (Cotoretigene Toliparvovec); A Control right eye; B Treated left eye; C Magnified image of the treated eye showing reversal of the hyperautofluorescent ring following RPGR gene therapy. D Assuming the exponential decay trajectory of the untreated right eye is mirrored by the left eye prior to treatment, the gain in autofluorescence demonstrated 6.2 years of recovery after treatment with Cotoretigene Toliparvovec.

AF ring total diameter data were plotted across time for all available datapoints. The proportion of variability in ring diameter attributable to time or baseline ring diameter was assessed using the coefficient of determination (R^2 value). A linear mixed model, with the dependent variable of total horizontal hyperautofluorescent ring width and independent variables of time, genotype and the interactions was used.

RESULTS

• **SUBJECTS:** Fifty-eight rod-cone dystrophy patients were analyzed in this study. None had syndromic disease. Analyzing hyperautofluorescent rings, 20 of these patients presented with early to mid-stage disease. The most common disease-causing genes in this cohort were *USH2A* (31.0%), *RPGR* (31.0%) and *RHO* (8.6%). Further details including patient molecular genetic testing can be found in supplementary Table 1 (available at https://www.aaojournal.org)

• **CROSS-SECTIONAL ANALYSIS:** The 3 distinct parameters of the hyperautofluorescent ring on FAF were strongly correlated with the anatomical measurements on OCT ($P < .001$) (Supplementary Table 2, available at https://www.aaojournal.org). The internal ring diameter, external ring diameter and ring thickness, were strongly correlated with the ellipsoid zone width ($r = 0.94$), external limiting membrane width ($r = 0.97$) and loss of the ellipsoid zone ($r = 0.92$), respectively in a variety of rod-cone dystrophies. The inner border of the ring corresponded to the region where the EZ terminates, whereas the area outside the ring is characterized by the absence of both the EZ and the external limiting membrane ELM, resulting in the outer nuclear layer being directly in contact with the RPE. Consequently, both structure and function remained intact within the hyperautofluorescent ring.

• **LONGITUDINAL ANALYSIS:** Early and mid-stage rings correlated with inner and outer photoreceptor segment loss and got smaller in diameter as the degeneration progressed (Figure 3). The results ($R^2 = 0.958$) suggested that FAF changes declined very predictably in a logarithmic fashion (Figure 4). Half-lives for *RPGR*, *USH2A* and *RHO* were 5.85, 19.75 and 23.42 years respectively ($P < .05$).

We identified 1 patient in Oxford who was previously reported by Lam et al study who had a particularly prominent fluorescent ring that could be monitored accurately at various points before and after gene therapy. The microperimetry of the treated eye in the patient demonstrated

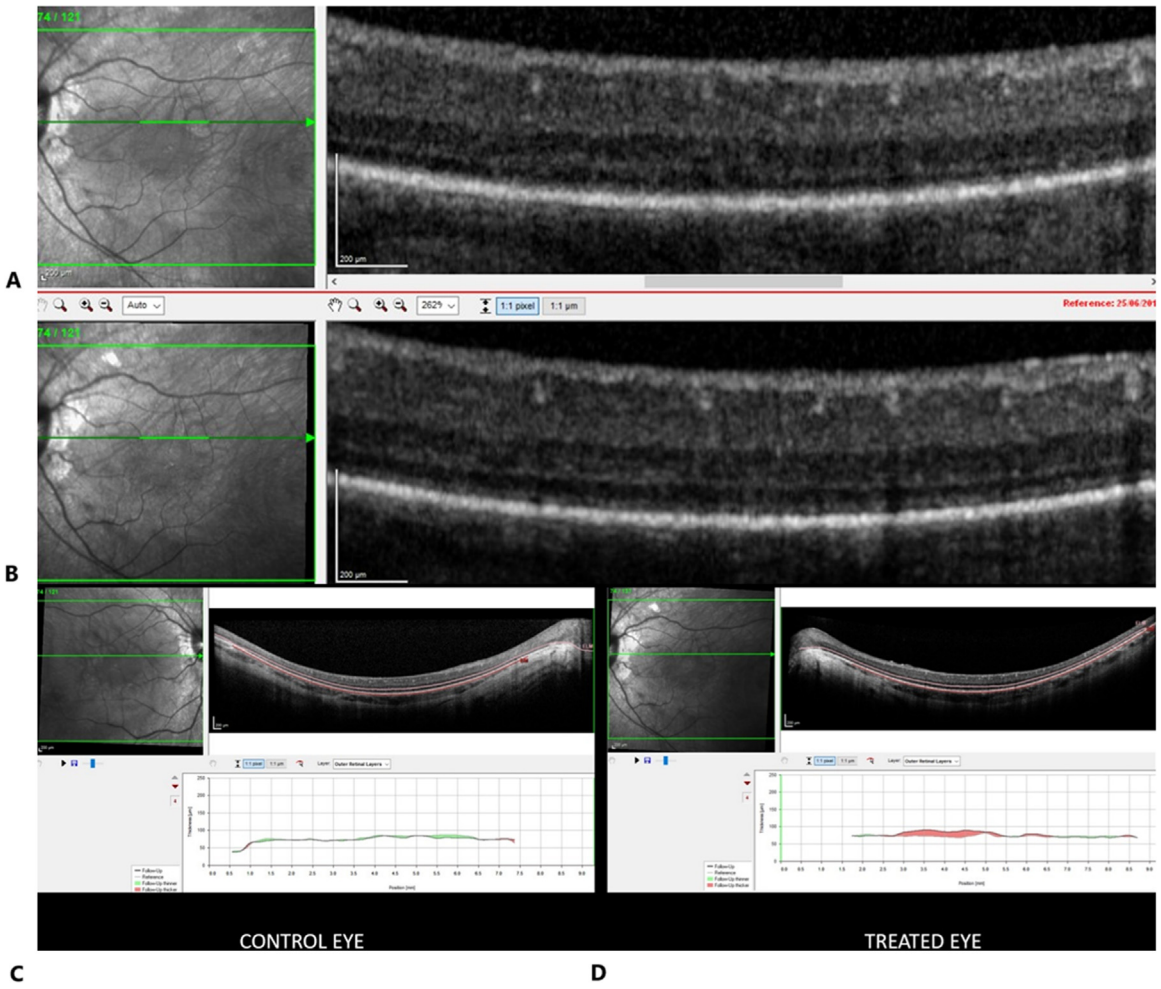

FIGURE 6. Multimodal imaging of a patient from the XIRIUS trial (Lam et al., 2024). OCT images of the right eye at (A) baseline and (B) three months post treatment with RPGR gene therapy shows evidence of regrowth of the external limiting membrane and increase in height of the outer segments after AAV8.coRPGR gene therapy with the correct full-length RPGR protein shows improved retinal anatomy. Segmentation of the OCT scans comparing the left eye (D) which was treated with RPGR gene therapy, to the right eye (C), which acted as the control, shows an increase in outer retinal thickness 3 months post RPGR gene therapy.

an increase in retinal sensitivity 3 months after RPGR gene therapy (using Cotoretigene Toliparvovec) compared to baseline (Figure 5A, B). Fundus autofluorescence images demonstrate reversal and expansion of the hyperautofluorescent ring diameter at this time point compared to baseline (Figure 5C). OCT scans show regeneration of the external limiting membrane and an increase in height of the outer segments 3 months after RPGR gene therapy (Figure 6A, B). Segmentation of the OCT scans comparing the left eye (treated with RPGR gene therapy) to the right eye (acting as control) show an increase in outer retinal thickness 3 months post RPGR gene therapy in the treated eye compared to the untreated eye which showed a decrease in outer retinal thickness (Figure 6C, D). This is quantifiable on segmented OCT scans. The microperimetry and multimodal imaging findings demonstrate anatomical reversal and a subsequent increase in retinal sensitivity 3 months after AAV8.coRPGR gene therapy with the correct full-length RPGR protein. In addition, heat maps were studied demonstrating that at 3 months post RPGR gene therapy (Figure 7B), a "red ring" appears in the left, treated eye in the intermediate zone (parafoveally). The right, control eye, shows further retinal thinning from baseline (Figure 7A). The emergence of the "red ring" on the heat maps correlates with the reversal of the hyperautofluorescent ring on AF scans.

DISCUSSION

In this study, we show a correlation between: the total hyperautofluorescent ring diameter and external limiting membrane zone width. Early and mid-stage rings correlated

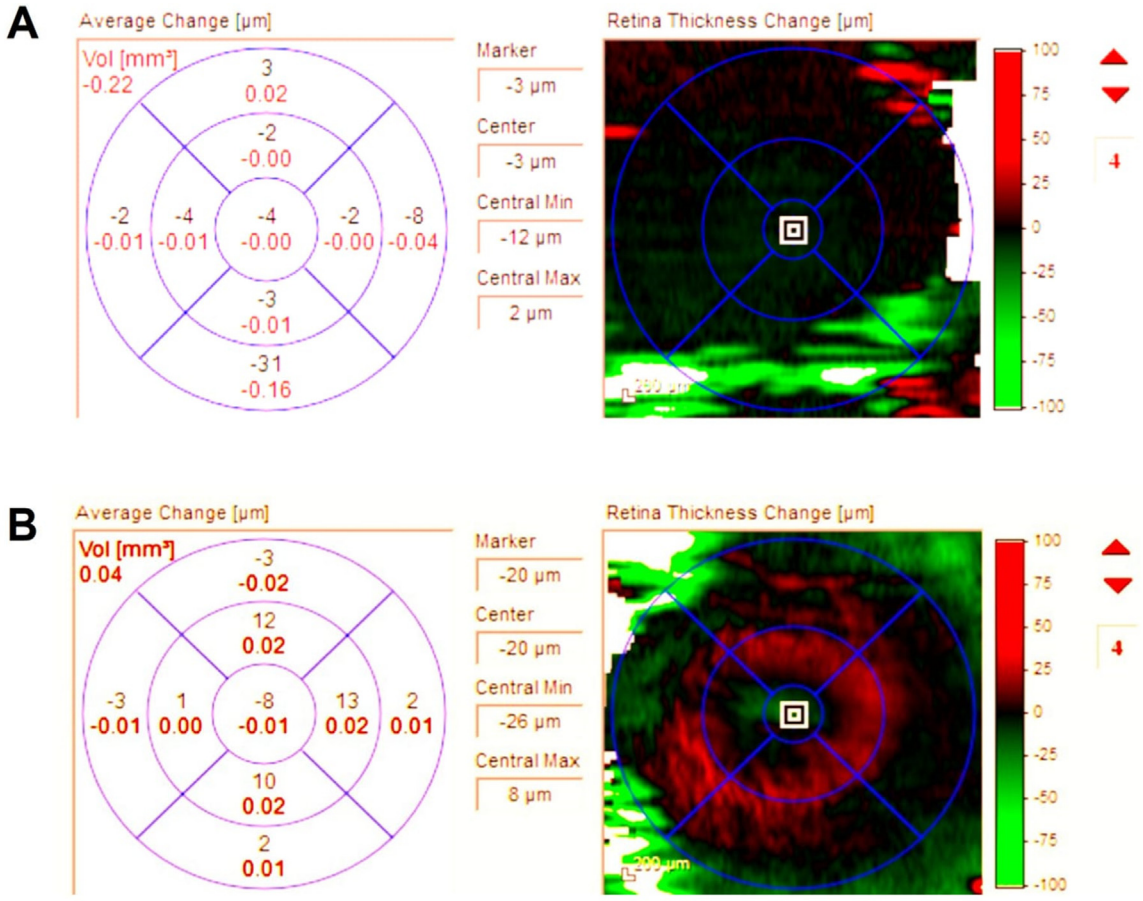

FIGURE 7. Heat maps (A) Right eye control, (B) Left treated eye. At 3 months post RPGR gene therapy, the "red ring" appears in the left, treated eye in the intermediate zone (parafoveally). The right, control eye, shows further retinal thinning from baseline. The emergence of the "red ring" on the heat maps correlates with reversal of the hyperautofluorescent ring on AF scans.

with inner and outer photoreceptor segment loss and get smaller as the degeneration progressed. Our results suggest that the diameter of the hyperautofluorescent ring declines predictably in a logarithmic fashion. Exponential decay appears to be consistent amongst individuals with rod-cone dystrophies, independent of genetic mutation—the larger or thicker the ring, the faster the degeneration. Individuals progressed at different rates and this is likely to depend on genetic, epigenetic, and environmental factors such as smoking and short-wave length light exposure.[15-17]

Our data extends prior work by showing that a structural, topographic biomarker (FAF ring diameter) can follow an exponential course and that the estimated time constant differs across genotypes in our dataset. Its value may extend beyond correlation with OCT structural parameters, especially due to its predictable longitudinal progression, and previous studies that confirm associations with functional outcomes. Berson and colleagues modelled mean annual exponential declines in dominant RP across visual acuity, visual field area, and ERG amplitude.[18] Long-term cone ERG decline has also been described as well-approximated by an exponential function over much of the disease course.[19] The "time constant" concept is directly analogous to the constant fractional loss per unit time used in those studies. One plausible explanation for the exponential course is the "one-hit" model of inherited neuronal death.[20] In this model, each vulnerable photoreceptor has an approximately constant probability of dying per unit time, which yields an exponential decline in surviving cells and in biomarkers that track them. This complements the geometric/topographic perspective in Figure 8: as surviving photoreceptors become spatially constrained, a roughly constant fractional loss can appear as a consistent fractional reduction in ring diameter over time.

The concept of FAF changes following an exponential decay function may be elucidated by examining the topographical arrangement of photoreceptors in the human retina (Figure 8).[21] The central fovea has the highest density of cones, ranging from 100 000 to 324 000 cones/mm^2. In contrast, the highest densities of rods reside in an elliptical ring at the eccentricity off the optic disc and extending into the nasal retina. The area with the highest density of rods is located in the superior mid-peripheral retina, whilst the lowest density is along the central horizontal meridian.

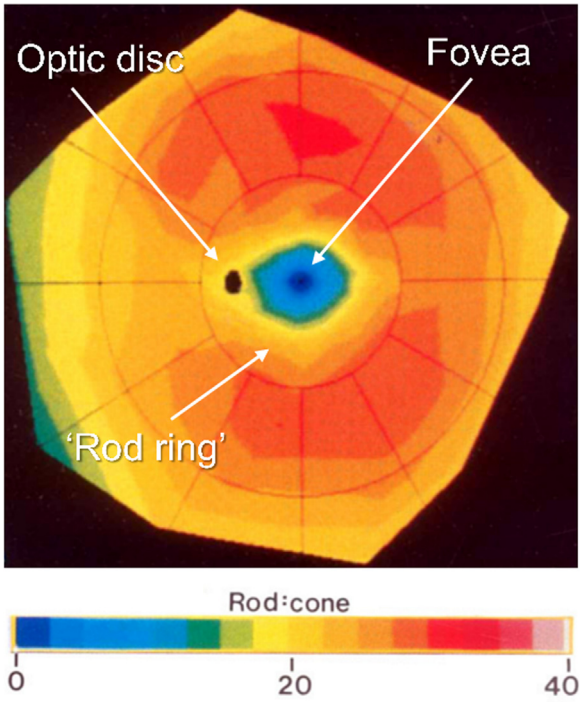

FIGURE 8. Topography map of average rod:cone ratios across the left retina. Each discrete colour in the colour bar represents a rod:cone ratio of 2.5, and the range of colours is 0-40. Lines of isoeccentricity in the overlying grid are at intervals of 5.94mm. Image adapted from Curcio et al., Human photoreceptor topography. J Comp Neurol: 1990

There is a subsequent decline in rod density on the leading edge of the rod ring. Within the "rod ring," the elongation of isodensity contours occurs along the horizontal meridian and are displaced inferiorly. Rod density increases most rapidly on the superior side of the rod-free zone and least rapidly along the horizontal meridian. Cone density falls steeply with increasing eccentricity from the foveal centre towards the rod ring. Hence, there appears to be an inherent interface where the rate of degeneration starts to decrease as it progresses towards the cone-rich zone, which is defined by the hyperautofluorescent ring. Furthermore, the bull's eye shape of the hyperautofluorescent ring can be attributed to eccentricity-dependent variations in rod-cone ratios as demonstrated in the image above.

These data support measurement of the FAF ring diameter as a potential novel biomarker for clinical trials in rod-cone dystrophies due to their significant correlation with OCT measurements. It is a practical structural endpoint for rare disease studies, mapping changes in progression over time. For clinical trials, the rate of progression may allow quantification of treatment effects by comparing the half-life of the decay function in treated individuals with the predicted untreated half-life. This is of particular value for patients with early rod-cone dystrophies in whom normal visual acuity is expected and in whom a ceiling effect prevents further functional improvement using visual acuity as an outcome measure. In gene therapy clinical trials, one eye often serves as a control whilst the contralateral eye receives treatment. Assuming that disease progression is symmetric between the eyes, this affords an opportunity to cf the treated eye to a near-ideal control. Early studies have suggested that a feature of retinitis pigmentosa is the symmetrical development of pigmentation and have reported a high degree of symmetry as assessed by visual fields.[22,23] More recent studies have additionally demonstrated a high degree of symmetry,[24,25] and bilateral concordance of the fundus hyperautofluorescent ring specifically. Although disease asymmetry can occur, these are observed less frequently (10-14.3%). When stratifying disease asymmetry by genotype, it is more frequently identified in *Rho* and *RP1*-associated rod-cone dystrophies.[26] Within the patient cohort we present in this study, 5 individuals had *RP1*- associated rod-cone dystrophies. In the case presented here, whereby the hyperautofluorescent ring is reversed following gene therapy (Figure 9, available at https://www.aaojournal.org), it is essential to consider ocular symmetry in RPGR-associated retinopathies in particular. It has been found that *RPGR*-associated retinopathies exhibit a strong similarity in retinal structure and function between eyes, supporting the use of the fellow eye as a near-ideal internal control in interventional trials.[27] Furthermore, a recent study noted that photoreceptors at the edge of the degeneration may regrow outer segment processes following successful gene therapy, resulting in some reversal of visual field loss[28] and in the Phase I/II clinical trial data,[29] it was noted that patients exhibited a significant and sustained improvement in retinal sensitivity and anatomy. In this study, we report more detailed findings of 1 patient from the above study. To the best of our knowledge, this data represents the first evidence of regrowth of the ELM after RPGR, or indeed any, gene therapy. Having defined the parameters of the ring in terms of the outer segment structure, we now explain how this changes following gene therapy and regrowth of photoreceptor outer segment. Not only was the progression of the FAF ring halted at 3 months, but there was an anatomical reversal of the FAF ring with RPGR gene therapy. The 'red ring' sign on heat maps provides evidence of regeneration of photoreceptor outer segments. This outer segment regeneration phenomenon was likely present in early animal models in which ciliopathies were treated for gene therapy, but were not detectable as OCT was not available.

The parameters of the FAF ring may indicate a specific area where the regeneration of photoreceptor outer segments, and hence the reversal of vision field loss, is most probable after gene therapy. The FAF ring could serve as a valuable marker for selecting participants in clinical trials, as it can identify individuals with a higher likelihood of responding well to treatment. Significantly, the FAF ring serves as a definitive marker for assessing the progression of photoreceptor degeneration or the regeneration of photoreceptor outer segments after therapeutic intervention. Fur-

thermore, in the clinical setting, having information on an individual's half-life would be of prognostic value and aid in providing genetic counseling for affected individuals. Notably, regulatory agencies are increasingly accepting structural outcome measures. This is evidenced by the validation of intraocular pressure measurement in glaucoma studies,[30] and fundal autofluorescence metrics in geographic atrophy clinical trials.[31]

The ring is a transition zone, and thickness may reflect the extent of partially stressed photoreceptors/RPE. RPE shape will change when the outer segment is lost and discs are no longer being shed however, the correlation with photoreceptors that we see in relation to the ring, demonstrates no obvious change on imaging in relation to the RPE structure. In our analysis, the primary longitudinal endpoint was external ring diameter (the boundary marker we could track most reliably over time). We did not model thickness longitudinally. This is a limitation, and future work with standardized FAF or dedicated segmentation methods could test whether thickness adds prognostic value beyond diameter. In addition, associations between microperimetry and structural OCT measures were not performed here due to small sample sizes but warrants further investigations.

We are now collecting datasets across the participating centers involved in the trial in order to quantify ring diameter/area and EZ metrics longitudinally in the larger treated cohort (with appropriate controls where available). This will allow us to determine (1) how many treated eyes show ring expansion and/or outer retinal structural improvement, (2) the time course of any changes, and (3) whether these changes relate to baseline phenotype, dose, or other factors.

To conclude, individuals with rod-cone dystrophies such as *RPGR*-related retinitis pigmentosa exhibit the presence of a hyperautofluorescent ring. This ring progresses over time following an exponential decay pattern. This is of crucial importance since it indicates that individuals possess a consistent half-life constant, which can be calculated by measuring the horizontal diameter of the FAF ring over a specific period. The FAF ring, therefore, serves as a potential endpoint to measure photoreceptor degeneration. This study also provides early evidence that AAV8.coRPGR gene therapy, with the correct full-length RPGR protein achieved by codon-optimization of the transgene, may reverse to some extent the progression of retinal degeneration. This is illustrated by the emergence of the 'red ring' sign. The results of anatomical reversal using the truncated RPGR protein have not yet been reported.[29]

CREDIT AUTHORSHIP CONTRIBUTION STATEMENT

MARAM E.A. ABDALLA ELSAYED: Writing – original draft, Methodology, Data curation. **AMANDEEP S. JOSAN:** Writing – review & editing, Formal analysis. **SALWAH REHMAN:** Writing – original draft, Data curation. **ROBERT E. MACLAREN:** Writing – review & editing, Validation, Methodology, Conceptualization.

Funding/Support: Robert E MacLaren reports financial support was provided by National Institute for Health Research (NIHR) Oxford Biomedical Research Centre. Maram E A Abdalla Elsayed reports financial support was provided by Foundation Fighting Blindness Clinical Research Fellowship Award.

Financial Disclosures: The authors declare the following financial interests/personal relationships which may be considered as potential competing interests: Robert E MacLaren reports financial support was provided by National Institute for Health Research (NIHR) Oxford Biomedical Research Centre. Robert E MacLaren has patent #US20180273594A1 issued to University of Oxford. If there are other authors, they declare that they have no known competing financial interests or personal relationships that could have appeared to influence the work reported in this paper.

REFERENCES

1. Robson A.G., Egan C., Holder G.E., Bird A.C., Fitzke F.W. Comparing rod and cone function with fundus autofluorescence images in Retinitis Pigmentosa. In; 2003:41-47. doi:10.1007/978-1-4615-0067-4_6
2. Lenassi E, Troeger E, Wilke R, Hawlina M. Correlation between macular morphology and sensitivity in patients with retinitis pigmentosa and hyperautofluorescent ring. *Investigat Opthalmol Visual Sci*. 2012;53(1):47. doi:10.1167/iovs.11-8048.
3. Robson AG, Lenassi E, Saihan Z, et al. Comparison of Fundus autofluorescence with photopic and scotopic fine matrix mapping in patients with retinitis pigmentosa: 4- to 8-year follow-up. *Investigat Opthalmol Visual Sci*. 2012;53(10):6187. doi:10.1167/iovs.12-10195.
4. Lima LH, Burke T, Greenstein VC, et al. Progressive constriction of the hyperautofluorescent ring in Retinitis Pigmentosa. *Am J Ophthalmol*. 2012;153(4):718–727 727.e1-2. doi:10.1016/j.ajo.2011.08.043.
5. Lee J, Asano S, Inoue T, et al. Investigating the usefulness of fundus autofluorescence in Retinitis Pigmentosa. *Ophthalmol Retina*. 2018;2(10):1062–1070. doi:10.1016/j.oret.2018.03.007.
6. Robson AG, Tufail A, Fitzke F, et al. Serial imaging and structure-function correlates of high-density rings of fundus autofluorescence in Retinitis Pigmentosa. *Retina*. 2011;31(8):1670–1679. doi:10.1097/IAE.0b013e318206d155.
7. Miere A, Le Meur T, Bitton K, et al. Deep learning-based classification of inherited retinal diseases using fundus autofluorescence. *J Clin Med*. 2020;9(10):3303. doi:10.3390/jcm9103303.

8. Aylward JW, Xue K, Patrício MI, et al. Retinal degeneration in choroideremia follows an exponential decay function. *Ophthalmology*. 2018;125(7):1122–1124. doi:10.1016/j.ophtha.2018.02.004.
9. Charng J, Escalona IA V, Turpin A, et al. Nonlinear reduction in hyperautofluorescent ring area in Retinitis Pigmentosa. *Ophthalmol Retina*. 2024;8(3):298–306. doi:10.1016/j.oret.2023.09.015.
10. Kupers ER, Benson NC, Carrasco M, Winawer J. Asymmetries around the visual field: from retina to cortex to behavior. *PLoS Comput Biol*. 2022;18(1):e1009771. doi:10.1371/journal.pcbi.1009771.
11. Carrasco MP, Talgar C, Cameron EL. Characterizing visual performance fields: effects of transient covert attention, spatial frequency, eccentricity, task and set size. *Spat Vis*. 2001;15(1):61–75. doi:10.1163/15685680152692015.
12. Cameron EL, Tai JC, Carrasco M. Covert attention affects the psychometric function of contrast sensitivity. *Vision Res*. 2002;42(8):949–967. doi:10.1016/S0042-6989(02)00039-1.
13. Barbot A, Xue S, Carrasco M. Asymmetries in visual acuity around the visual field. *J Vis*. 2021;21(1):2. doi:10.1167/jov.21.1.2.
14. Mackeben M. Sustained focal attention and Peripheral letter recognition. *Spat Vis*. 1999;12(1):51–72. doi:10.1163/156856899X00030.
15. Campochiaro PA, Mir TA. The Mechanism of cone cell death in retinitis pigmentosa. *Prog Retin Eye Res*. 2018;62:24–37. doi:10.1016/j.preteyeres.2017.08.004.
16. Oishi A, Noda K, Birtel J, et al. Effect of smoking on macular function and retinal structure in Retinitis Pigmentosa. *Brain Commun*. 2020;2(2):fcaa117. doi:10.1093/braincomms/fcaa117.
17. Orlans HO, Merrill J, Barnard AR, Charbel Issa P, Peirson SN, MacLaren RE. Filtration of short-wavelength light provides therapeutic benefit in retinitis pigmentosa caused by a common rhodopsin mutation. *Invest Ophthalmol Vis Sci*. 2019;60(7):2733–2742. doi:10.1167/iovs.19-26964.
18. Berson EL, Rosner B, Weigel-DiFranco C, Dryja TP, Sandberg MA. Disease progression in patients with dominant Retinitis Pigmentosa and Rhodopsin mutations. *Invest Ophthalmol Vis Sci*. 2002;43(9):3027–3036.
19. Berson EL. Long-term visual prognoses in patients with retinitis pigmentosa: the Ludwig von Sallmann Lecture. *Exp Eye Res*. 2007;85(1):7–14. doi:10.1016/j.exer.2007.03.001.
20. Clarke G, Collins RA, Leavitt BR, Andrews DF, Hayden MR, Lumsden CJ, McInnes RR. A One-hit model of cell death in inherited neuronal degenerations. *Nature*. 2000;406(6792):195–199. doi:10.1038/35018098.
21. Spaide RF, Curcio CA. Anatomical correlates to the bands seen in the outer retina by optical coherence tomography. *Retina*. 2011;31(8):1609–1619. doi:10.1097/IAE.0b013e3182247535.
22. Biro I. Symmetrical development of pigmentation as a specific feature of the fundus pattern in Retinitis Pigmentosa. *Am J Ophthalmol*. 1963;55:1176–1179.
23. Massof RW, Finkelstein D, Starr SJ, Kenyon KR, Fleischman JA, Maumenee IH. Bilateral symmetry of vision disorders in typical Retinitis Pigmentosa. *Br J Ophthalmol*. 1979;63(2):90–96. doi:10.1136/bjo.63.2.90.
24. Sujirakul T, Davis R, Erol D, et al. Bilateral concordance of the Fundus hyperautofluorescent ring in typical retinitis pigmentosa patients. *Ophthalmic Genet*. 2015;36(2):113–122. doi:10.3109/13816810.2013.841962.
25. Fakin A, Jarc-Vidmar M, Glavač D, Bonnet C, Petit C, Hawlina M. Fundus autofluorescence and optical coherence tomography in relation to visual function in usher syndrome type 1 and 2. *Vision Res*. 2012;75:60–70. doi:10.1016/j.visres.2012.08.017.
26. Jauregui R, Chan L, Oh JK, Cho A, Sparrow JR, Tsang SH. Disease asymmetry and hyperautofluorescent ring shape in Retinitis Pigmentosa patients. *Sci Rep*. 2020;10(1):3364. doi:10.1038/s41598-020-60137-9.
27. Bellingrath JS, Ochakovski GA, Seitz IP, et al. High symmetry of visual acuity and visual fields in *RPGR* -linked retinitis pigmentosa. *Investigat Opthalmol Visual Sci*. 2017;58(11):4457. doi:10.1167/iovs.17-22077.
28. Cehajic-Kapetanovic J, Xue K, Martinez-Fernandez de la Camara C, et al. Initial results from a First-in-human gene therapy trial on X-linked Retinitis Pigmentosa Caused by mutations in RPGR. *Nat Med*. 2020;26(3):354–359. doi:10.1038/s41591-020-0763-1.
29. Lam BL, Pennesi ME, Kay CN, et al. Assessment of visual function with Cotoretigene Toliparvovec in X-linked retinitis pigmentosa in the randomized XIRIUS phase 2/3 study. *Ophthalmology*. 2024. doi:10.1016/j.ophtha.2024.02.023.
30. Garway-Heath DF, Crabb DP, Bunce C, et al. Latanoprost for open-angle glaucoma (UKGTS): a randomised, multicentre, placebo-controlled trial. *Lancet*. 2015;385(9975):1295–1304. doi:10.1016/S0140-6736(14)62111-5.
31. Heier JS, Lad EM, Holz FG, et al. Pegcetacoplan for the treatment of geographic atrophy secondary to age-related macular degeneration (OAKS and DERBY): two multicentre, randomised, double-masked, sham-controlled, phase 3 trials. *Lancet*. 2023;402(10411):1434–1448. doi:10.1016/S0140-6736(23)01520-9.